doi:10.1093/jmcb/mjy074
Published online December 7, 2018

Article

AFF3-DNA methylation interplay in maintaining the mono-allelic expression pattern of *XIST* in terminally differentiated cells

Yue Zhang[1], Chao Wang[1], Xiaoxu Liu[1], Qian Yang[1], Hongliang Ji[1], Mengjun Yang[1], Manman Xu[1], Yunyan Zhou[1], Wei Xie[1,2], Zhuojuan Luo[1,2,*], and Chengqi Lin[1,2,*]

[1] Institute of Life Sciences, The Key Laboratory of Developmental Genes and Human Disease, Southeast University, Nanjing 210096, China
[2] Co-innovation Center of Neuroregeneration, Nantong University, Nantong 226001, China
* Correspondence to: Chengqi Lin, E-mail: cqlin@seu.edu.cn; Zhuojuan Luo, E-mail: zjluo@seu.edu.cn

Edited by Zhiyuan Shen

X chromosome inactivation and genomic imprinting are two classic epigenetic regulatory processes that cause mono-allelic gene expression. In female mammals, mono-allelic expression of the long non-coding RNA gene *X-inactive specific transcript* (*XIST*) is essential for initiation of X chromosome inactivation upon differentiation. We have previously demonstrated that the central factor of super elongation complex-like 3 (SEC-L3), AFF3, is enriched at gamete differentially methylated regions (DMRs) of the imprinted loci and regulates the imprinted gene expression. Here, we found that AFF3 can also bind to the DMR downstream of the *XIST* promoter. Knockdown of AFF3 leads to de-repression of the inactive allele of *XIST* in terminally differentiated cells. In addition, the binding of AFF3 to the *XIST* DMR relies on DNA methylation and also regulates DNA methylation level at DMR region. However, the KAP1-H3K9 methylation machineries, which regulate the imprinted loci, might not play major roles in maintaining the mono-allelic expression pattern of *XIST* in these cells. Thus, our results suggest that the differential mechanisms involved in the *XIST* DMR and gDMR regulation, which both require AFF3 and DNA methylation.

Keywords: AFF3, *XIST*, X chromosome inactivation, DNA methylation

Introduction

In mammals, females (XX) have two copies of gene-rich X chromosomes, while males (XY) have only one copy of X chromosome and one copy of gene-poor Y chromosome. X chromosome inactivation (XCI) is a regulated developmental process by which mammalian females can silence one of the two X chromosomes, thus offsetting X-linked gene dosage imbalance between males and females (Lyon, 1961). The long non-coding RNA (lncRNA) *XIST/Xist* is expressed exclusively from the inactive X chromosome (Xi) and essential for initiation of XCI (Borsani et al., 1991; Brockdorff et al., 1991; Brown et al., 1991). Cis accumulation of *XIST/Xist* RNA on the X chromosome leads to chromosome wide heterochromatinization and gene silencing (Augui et al., 2011; Lee and Bartolomei, 2013).

One of the main tasks for dissecting the XCI process is to identify factors that regulate the expression of *XIST/Xist* gene. In murine pluripotent stem cells, *Xist* expression in repressed; while upon differentiation, *Xist* is randomly activated from either of the two X chromosomes in female, triggering inactivation of the *Xist* expressed X chromosome. The *Xist* gene on the active X chromosome remains 'off' status (Navarro et al., 2005; Sun et al., 2006). Several factors have been identified in regulating the *Xist* gene expression, and most of these factors are encoded within the X-Inactivation Center (XIC), which is located on X chromosome, encompassing the *Xist* gene, and controlling X chromosome inactivation. For example, the non-coding gene *TSIX/Tsix* within XIC is antisense to *XIST/Xist*. Although it has been demonstrated that human *TSIX* is not functional in *XIST* repression, murine *Tsix* has been shown to negatively regulate the expression and accumulation of *Xist* in cis (Lee and Lu, 1999; Migeon et al., 2002; Navarro et al., 2005; Sun et al., 2006). In contrast, the non-coding transcripts *Jpx* and *Ftx* within XIC are involved in *Xist* activation (Tian et al., 2010; Chureau et al., 2011). Upon differentiation, the E3 ubiquitin ligase RNF12 encoded by an X-linked gene within XIC is upregulated and targets the *Xist* repressor REX1 to degradation, therefore favoring

Received July 18, 2018. Revised October 15, 2018. Accepted November 20, 2018.

Xist gene expression (Jonkers et al., 2009; Gontan et al., 2012). The zinc finger protein YY1 is a recently identified autosomal factor that binds to the unmethylated *XIST/Xist* promoter CpG island and directly activates the *XIST/Xist* promoter in both human and mouse (Makhlouf et al., 2014). Most of these studies focus on transcriptional regulation of the *XIST/Xist* gene at the onset of XCI following differentiation, while less is known about *XIST/Xist* regulation in terminally differentiated cells. In addition, a plethora of recent studies suggest that the *XIST* gene is dysregulated in various human cancers. It has been reported that *XIST* RNA can act as a tumor suppressor or activator in many cancers (Yildirim et al., 2013; Chen et al., 2017). Thus, the *XIST* gene is involved in important physiological and pathological processes. Therefore, it is essential to further explore the underlying mechanisms by which the mono-allelic expression pattern of *XIST* is maintained.

XCI and genomic imprinting are two classic epigenetic regulatory processes to ensure the mono-allelic expression of their target genes. These two processes are united by allelic control of gene expression in large chromatin domain by cis-acting master regulatory region (Lee and Bartolomei, 2013). We recently demonstrated that the central factor of super elongation complex-like 3 (SEC-L3), AFF3, is recruited to the gamete differentially methylated regions (gDMRs) of imprinted loci by the scaffold protein TRIM28 and its related heterochromatin H3K9 methylation machinery, and to the unmethylated enhancer of imprinted locus by Kruppel like zinc finger protein ZFP281, to regulate the expression of imprinted genes (Luo et al., 2016; Wang et al., 2017). In this study we found that AFF3 can also bind to the 5′ differentially methylated region (DMR) downstream of the *XIST* promoter and repress its expression in terminally differentiated cells. In contrast, the H3K9 methylation machineries, which are involved in genomic imprinting regulation, seem not to play major roles in *XIST* gene repression in these cells. In addition, the recruitment of AFF3 to the *XIST* 5′ promoter DMR is not dependent on H3K9 methylation machineries, but rely on the methylation status of the *XIST* DMR.

Results

AFF3 is required for the silencing of XIST in terminally differentiated cells

We have previously reported that the central factor of SEC-L3, AFF3, can bind to the master control regions of genomic imprinted loci and regulate the expression of imprinted genes (Luo et al., 2016). Since many similarities have been identified between the regulation of imprinted genes and the XCI master gene, *XIST*, we investigated the potential involvement of AFF3 in *XIST* gene expression. We first analyzed our previously published RNA-Seq datasets from HEK293T cells bearing control or AFF3 specific shRNA (Luo et al., 2012). The expression of XIST is upregulated following shRNA-mediated AFF3 knockdown (Figure 1A and B). To further validate this phenomenon, we conducted quantitative real-time PCR analysis after knockdown of AFF3 using an independent shRNA. Data confirmed that AFF3 knockdown increases XIST transcripts (Figure 1C and D).

We next asked whether increased XIST expression in AFF3-depleted HEK293T cells affects the formation of XIST RNA cloud on the inactive X chromosome (Xi). Control and AFF3-depleted cells were hybridized with fluorescent XIST RNA probes. HEK293T is a hypotriploid human female cell line, containing three copies of X chromosomes, two of which are inactive and the rest one is active. Our XIST RNA FISH also showed that the most majority of HEK293T cells contain two XIST RNA clouds within a single nucleus (Figure 1E and Supplementary Figure S1A). Consistent with the qPCR data, AFF3 knockdown leads to an increase in the number of cells with three XIST RNA clouds (Figure 1E and F; Supplementary Figure S1A).

The effects on XIST silencing after AFF3 knockdown were repeated in IMR-90 cells, which were derived from the lung of a female fetus. IMR-90 cells have a normal diploid karyotype with 46 chromosomes (46, XX), which could provide a closer condition to mimic a real function of AFF3 in XIST regulation *in vivo*. In line with the observation in HEK293T cells, knockdown of AFF3 in IMR-90 using two independent shRNAs against AFF3 also leads to an increase of XIST transcripts (Figure 1G and H; Supplementary Figure S1B and C). By FISH for XIST RNA, we observed that more than 98% of the diploid female fibroblasts IMR-90 displayed a single XIST RNA cloud (Figure 1I). AFF3 knockdown in IMR-90 leads to an increase in the number of cells with two XIST RNA clouds (Figure 1I and J). Therefore, from both cases we concluded that AFF3 inhibits XIST transcription and that AFF3 is involved in the maintenance of a proper X chromosome inactive state in female cells.

AFF3 binds to the methylated allele of XIST in female cells

It has been shown that AFF3 can bind to the methylated gDMRs within the CpG islands of imprinted loci to regulate the expression of imprinted genes (Luo et al., 2016). Similar to imprinted genes, the *XIST* gene promoter CpG island is methylated on the active X chromosome (Xa), and unmethylated on Xi (Heard et al., 1993). We thus speculated that AFF3 regulates the expression of *XIST* gene through directly binding to the differentially methylated *XIST* promoter CpG island, hereinafter referred to as the *XIST* DMR. Quantitative PCR after chromatin immunoprecipitation (ChIP-qPCR) demonstrates that AFF3 is associated with the *XIST* DMR in both IMR-90 and HEK293T (Figure 2A–C). Pol II ChIP-qPCR in HEK293T at the *XIST* DMR and the *GAPDH* gene promoter region was performed as positive controls (Supplementary Figure S2A and B). To address whether AFF3 binds to the methylated allele, we performed methylated DNA immunoprecipitation (MeDIP) assay after AFF3 ChIP in HEK293T. The result demonstrated that the AFF3 bound *XIST* DMR is methylated (Figure 2D), suggesting that AFF3 has a binding preference for the methylated allele of *XIST* in female cells. To confirm the binding of AFF3 to the methylated allele of the *XIST* DMR, we further performed bisulfite-sequencing analysis of the *XIST* DMR from AFF3 ChIP DNA. AFF3 was found exclusively bound to the methylated allele of the *XIST* DMR (Figure 2A and E). This finding is also consistent with our previous finding that AFF3 is exclusively recruited to the

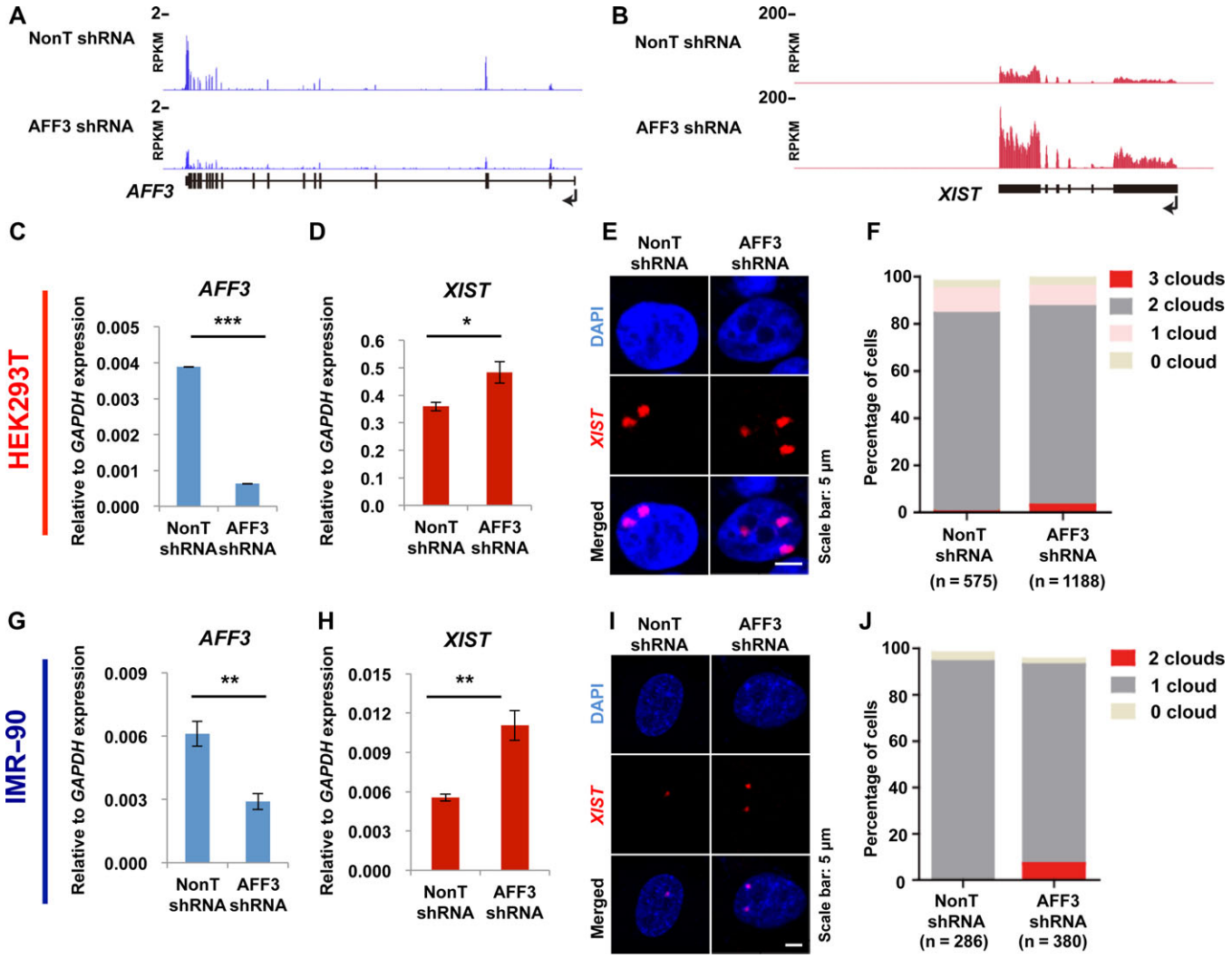

Figure 1 AFF3 is required for the silencing of *XIST* in terminally differentiated cells. (**A**) RNA-Seq showing the efficiency of shRNA-mediated AFF3 knockdown in HEK293T cells. (**B**) *XIST* RNA level increased by knockdown of AFF3 in HEK293T cells. (**A** and **B**) The y-axes represent RPKM values. RNA-Seq data in control and AFF3 knockdown HEK293T cells were downloaded from GSE34097. (**C**) RT-qPCR showing the efficiency of AFF3 knockdown by an independent shRNA in HEK293T cells. (**D**) RT-qPCR confirming the increase of *XIST* RNA level by an independent AFF3 shRNA in HEK293T cells. (**E**) *XIST* RNA FISH in control and AFF3 knockdown HEK293T cells. Scale bar, 5 μm. (**F**) Quantification of nuclei with *XIST* clouds in control and AFF3 knockdown HEK293T cells. The Chi-square test shows that the difference of cells containing three *XIST* clouds between control and AFF3 knockdown groups is significant. (**G**) RT-qPCR showing the efficiency of AFF3 knockdown in IMR-90 cells. (**H**) RT-qPCR showing an increase of *XIST* RNA level by AFF3 shRNA in IMR-90 cells. (**I**) *XIST* RNA FISH in control and AFF3 knockdown IMR-90 cells. Scale bar, 5 μm. (**J**) Quantification of nuclei with *XIST* clouds in control and AFF3 knockdown IMR-90 cells. The Chi-square test shows that the difference of cells containing two *XIST* clouds between control and AFF3 knockdown groups is significant. (**C**, **D**, **G**, and **H**) The expression of *AFF3* and *XIST* was normalized to the expression of *GAPDH*. Results shown are technical replicates from representative biological replicates. Error bars represent standard deviations. Significant differences are marked with asterisks (*t*-test, $*P < 0.05$; $**P < 0.01$; $***P < 0.001$).

methylated alleles of the DMR in the imprinted loci (Luo et al., 2016).

ENL and AF9, components of AFF3-containing complex SEC-L3, are also required for XIST silencing

The YEATS domain proteins ENL and AF9 are subunits of the AFF3-containing complex SEC-L3 (Luo et al., 2012). It has also been reported that ENL and AF9 can interact with the components within PRC1 and mediate gene repression (Ui and Yasui, 2016). Since we found AFF3 can suppress *XIST* transcription, we speculated that its interacting proteins ENL and AF9 might also play similar roles. To test this hypothesis, we first examined the requirement of ENL or AF9 in *XIST* gene repression by performing ENL or AF9 knockdown experiments in IMR-90 cells

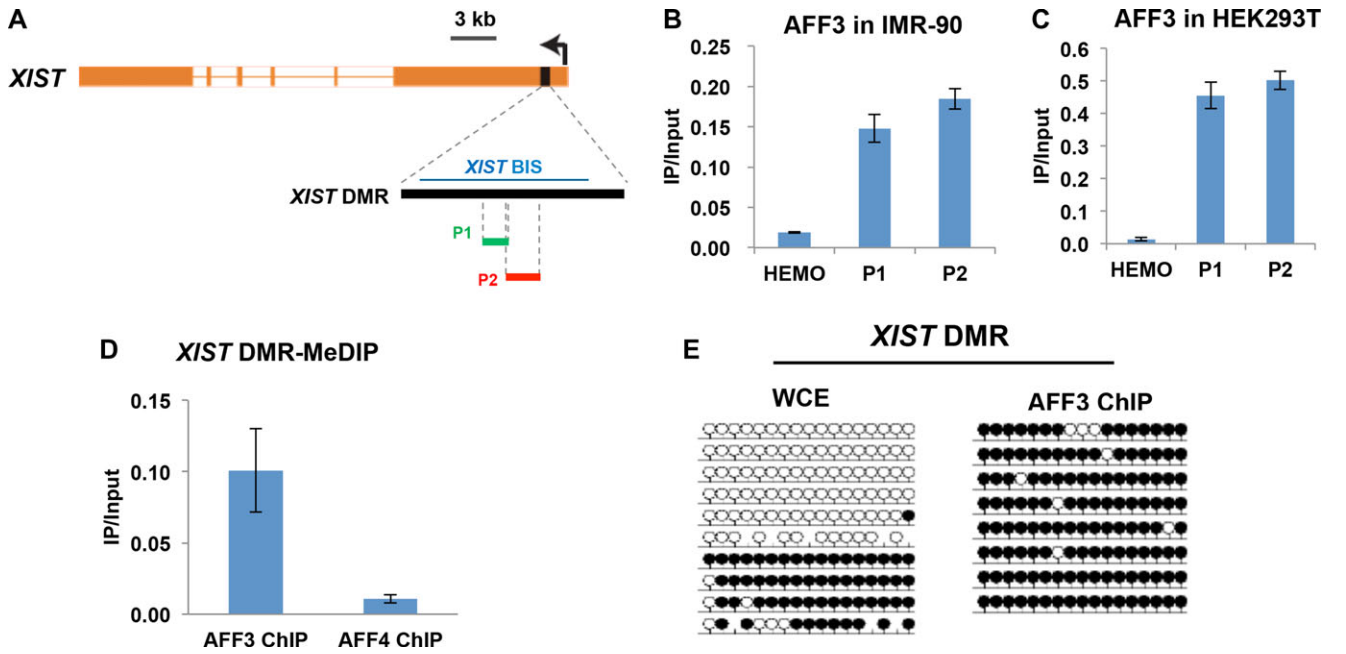

Figure 2 AFF3 binds to the methylated allele of *XIST* in female cells. (**A**) Schematic illustration of the location of the *XIST* CpG island/*XIST* DMR, the amplified genomic regions of the *XIST* DMR, and the amplified genomic region of the *XIST* DMR after bisulfite treatment. (**B** and **C**) AFF3 is recruited to the *XIST* DMR in HEK293T (**B**) and IMR-90 (**C**) cells used in ChIP assay. The nonexpressed β-globin gene (*HEMO*) served as a negative control. Error bars represent standard deviations. (**D**) AFF3 binds to the methylated allele of the *XIST* DMR. MeDIP assays were performed using AFF3 or AFF4 ChIP DNA in HEK293T cells. AFF4 ChIP DNA was used as a negative control for the MeDIP assay. Primer pair P2 was used to amplify the *XIST* DMR. The *HEMO* gene served as a negative control for ChIP-qPCR. Error bars represent standard deviations. (**E**) Bisulfite-sequencing analysis of whole-cell extract (WCE; input for AFF3 ChIP) and AFF3 ChIP in HEK293T at the *XIST* DMR. Methylated and unmethylated cytosines are designated by filled and unfilled circles, respectively. Each line indicates a unique DNA clone. In contrast to WCE, the AFF3 ChIP DNA is predominantly methylated at the *XIST* DMR.

(Supplementary Figure S3A and B). Knockdown of either ENL or AF9 leads to an increase in XIST RNA level (Figure 3A and B). ENL or AF9 knockdown in IMR-90 cells also results in an increase of the number of cells displaying two XIST RNA clouds, as shown by RNA FISH (Figure 3C and D). Our result further indicated that AF9 occupies the *XIST* DMR in IMR-90 cells by ChIP experiments (Figure 3E). Thus, it is highly possible that AF9 regulates *XIST* gene expression via its direct binding to the *XIST* DMR.

The recruitment of AFF3 to the XIST DMR is KAP1 independent

In the imprinted loci, AFF3 binds to the gDMRs that are both DNA and H3K9 methylated. KAP1 colocalizes with AFF3 and the H3K9 methyltransferase SETDB1 and recruits the two factors to the imprinted gDMRs (Quenneville et al., 2011; Luo et al., 2016). Here we performed AFF3 ChIP-Seq in HEK293T cells and compared the binding profile of AFF3, KAP1, and H3K9me3 across the *XIST* locus. Consistent with AFF3 ChIP-qPCR data, AFF3 is specifically located to the DMR downstream of the *XIST* promoter (Figure 4A). AFF3 and KAP1 co-occupy the gDMRs of the imprinted loci with H3K9me3. However, unlike AFF3, we found that KAP1 and H3K9me3 spread over the entire *XIST* gene, with no obvious peaks overlapping with the *XIST* DMR in both HEK293T and IMR-90 cells (Figure 4A and Supplementary Figure S4A). We also performed KAP1 ChIP in IMR-90 cells. In consistent with a previous study showing that KAP1 is enriched at paternal gDMRs in human cells, we found that KAP1 occupies the paternal MEG3 gDMR in IMR-90 cells (Tao et al., 2018). However, KAP1 is not detectable at the AFF3 occupied the *XIST* DMR in IMR-90 cells (Figure 4B). This suggests that the recruitment of AFF3 to the *XIST* DMR may not be mediated by KAP1. To test this hypothesis, we knockdowned KAP1 in IMR-90 cells. The efficiency of knockdown was confirmed by RT-qPCR and western blot (Figure 4C and Supplementary Figure S4B). We then performed AFF3 ChIP in IMR-90 cells depleted of KAP1. The occupancy of AFF3 at the *XIST* DMR is equally detected in both control and KAP1 knockdown cell line by ChIP-qPCR (Figure 4D). We also observed similar results in HEK293T cells (Supplementary Figure S4C). Thus, the data suggested that the recruitment of AFF3 to the *XIST* DMR is KAP1 independent in both IMR-90 and HEK293T cells.

Since KAP1 and H3K9me3 occupy the *XIST* locus, we further examined the formation of XIST clouds after the depletion of KAP1 and SETDB1. The efficiency of SETDB1 knockdown in IMR-90 cells was confirmed by RT-qPCR and western blot (Supplementary Figure S5A and B). FISH experiments demonstrate that the percentage of IMR-90 cells with two XIST clouds remains the same after KAP1 or SETDB1 knockdown, which is different from what has been observed after AFF3 knockdown (Figure 4E). This further indicates

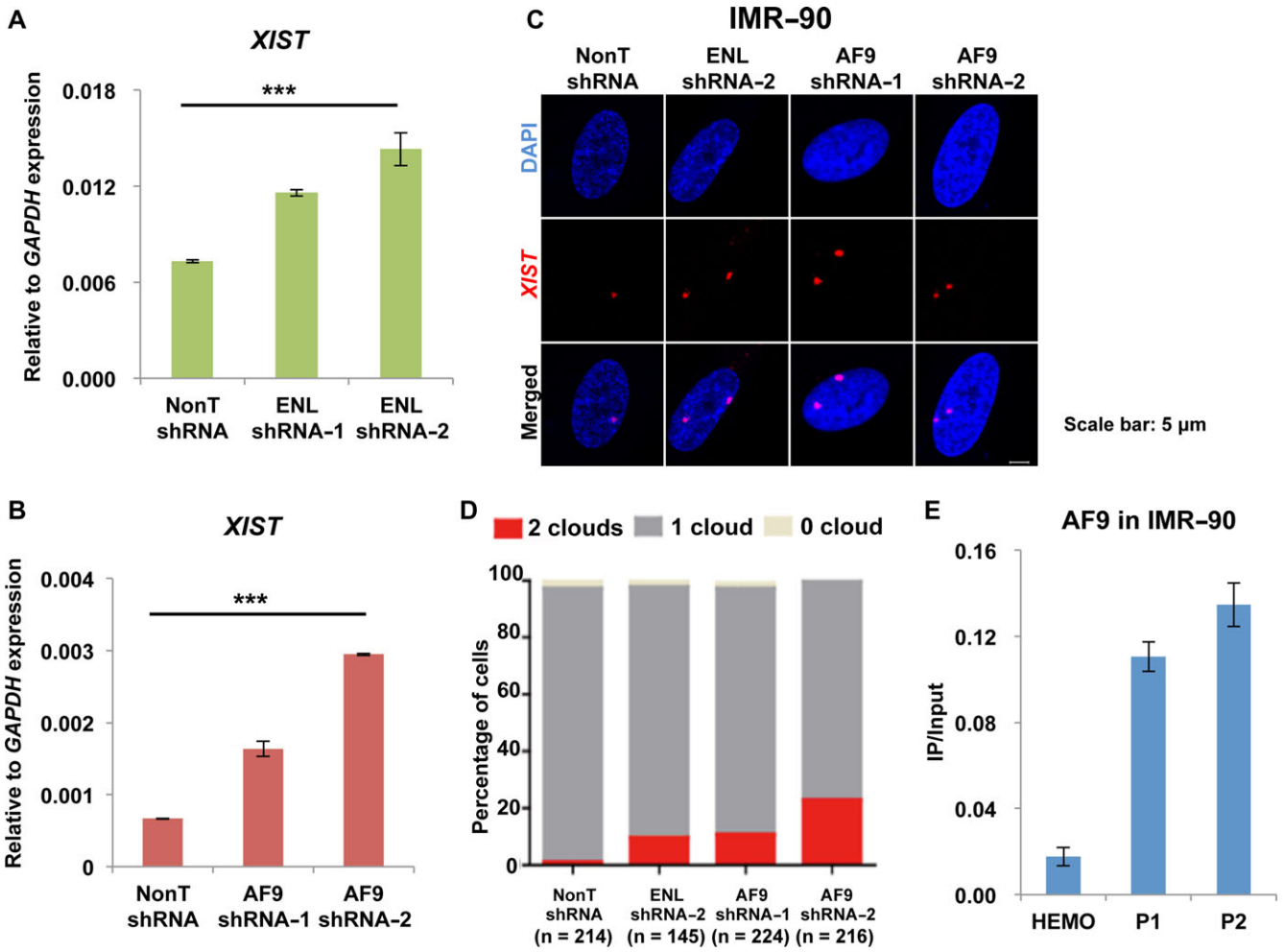

Figure 3 ENL and AF9, components of AFF3-containing complex SEC-L3, are also required for *XIST* silencing. (**A** and **B**) RT-qPCR showing an increase of *XIST* RNA level by ENL (**A**) or AF9 (**B**) shRNA in IMR-90 cells. The expression of *ENL* and *AF9* was normalized to the expression of *GAPDH*. Results shown are technical replicates from representative biological replicates. Error bars represent standard deviations. Significant differences are marked with asterisks (*t*-test, $*P < 0.05$; $**P < 0.01$; $***P < 0.001$). (**C**) *XIST* RNA FISH in control, ENL knockdown, or AF9 knockdown IMR-90 cells. Scale bar, 5 μm. (**D**) Quantification of nuclei with *XIST* clouds in control, ENL knockdown, or AF9 knockdown IMR-90 cells. The Chi-square test shows that the differences of cells containing two *XIST* clouds between control and ENL knockdown or AF9 knockdown groups are significant. (**E**) ChIP-qPCR showing that AF9 binds to the *XIST* DMR in IMR-90 cells. The *HEMO* gene served as a negative control for ChIP-qPCR. Error bars represent standard deviations.

that regulation of *XIST* gene expression by AFF3 is independent of KAP1 in IMR-90 cells.

In addition, we performed the knockdown of other H3K9 methyltransferase, such as SUV39H1, SUV39H2, and EHMT2 in IMR-90 cells. RT-qPCR analyses demonstrated that knockdown of these H3K9 methyltransferase does not lead to an obvious change of the *XIST* gene expression (Supplementary Figure S5C–F), suggesting that the H3K9 methylation machineries examined above might not be a major factor in regulating the mono-allelic expression of the *XIST* gene in the cells we tested.

The recruitment of AFF3 to the XIST DMR is DNA methylation dependent

It has been well established that DNA hypomethylation can activate *XIST* gene expression. The DNA demethylating agent 5-Aza-2′-deoxycytidine (5-aza) can lead to the demethylation of the *XIST* DMR and *XIST* reactivation in somatic cells (Hansen et al., 1998; Tinker and Brown, 1998; de Araujo et al., 2014). Since AFF3 can bind to the methylated *XIST* DMR and repress *XIST* gene expression, we speculated that the binding of AFF3 might rely on the methylation status of the *XIST* DMR. To test this hypothesis, we treated IMR-90 cells with 5-aza and then performed AFF3 ChIP. 5-aza application leads to an ~50% increase of *XIST* gene expression and percentage of cells with two XIST clouds in IMR-90 cells (Figure 5A–C). The occupancy of AFF3 at the *XIST* DMR is reduced ~40% in IMR-90 cells after 5-aza treatment (Figure 5D). We then examined the requirement of DNA methylation for the binding of AFF3 to the *XIST* DMR in HEK293T cells. Consistently, 5-aza treatment in HEK293T results in an increase in *XIST* gene expression and loss of AFF3 binding

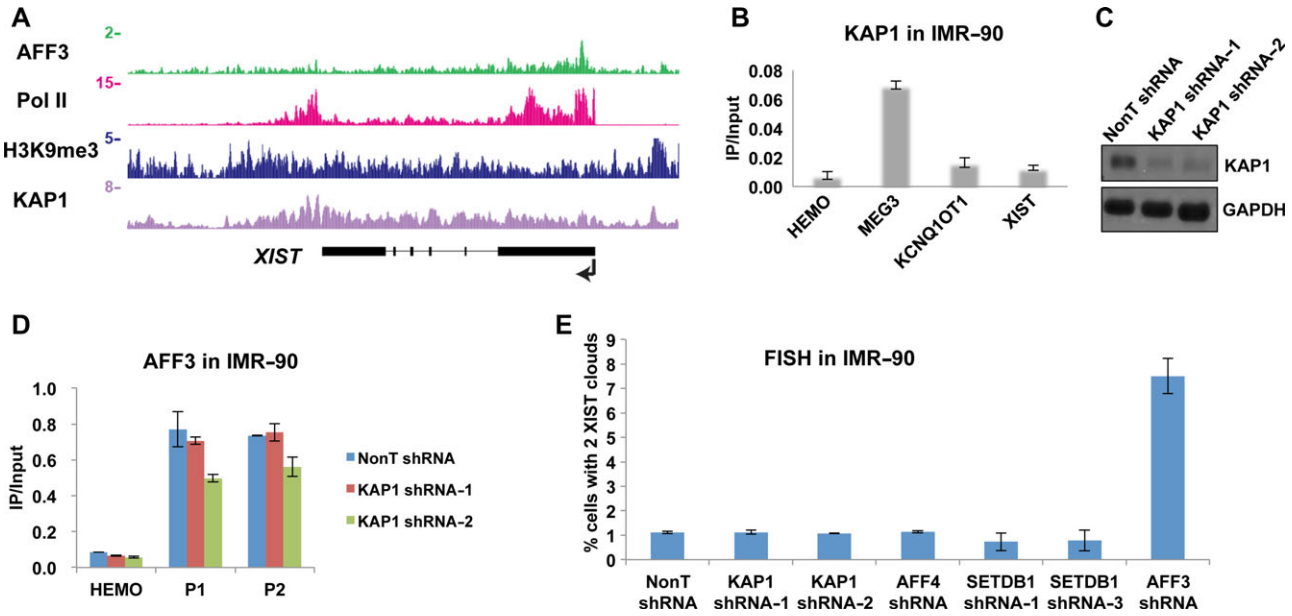

Figure 4 The recruitment of AFF3 to the *XIST* DMR is KAP1 and H3K9 methylation machineries independent. (**A**) ChIP-Seq showing AFF3, Pol II, H3K9me3, and KAP1 occupancies at the *XIST* locus in HEK293T cells. Pol II ChIP-Seq data were downloaded from GSE34097. H3K9me3 and KAP1 ChIP-Seq data were obtained from Encode project. (**B**) ChIP-qPCR showing that KAP1 is enriched in the paternal *MEG3* gDMR, but not the AFF3 bound *XIST* DMR in IMR-90 cells. The *HEMO* gene served as a negative control for ChIP-qPCR. Error bars represent standard deviations. (**C**) Knockdown of KAP1 by lentiviral-mediated shRNA in IMR-90 cells. KAP1 protein levels were measured by western blotting. GAPDH was used as a loading control. (**D**) ChIP-qPCR showing that the occupancy of AFF3 at the *XIST* DMR remains unchanged after KAP1 knockdown in IMR-90 cells. The *HEMO* gene served as a negative control for ChIP-qPCR. Error bars represent standard deviations. (**E**) Quantification of nuclei with XIST clouds in control, KAP1 knockdown, AFF4 knockdown, SETDB1 knockdown, or AFF3 knockdown IMR-90 cells.

to the *XIST* DMR (Figure 5E and F). We also analyzed the effects of AFF3 on DNA methylation status of the *XIST* DMR by performing bisulfite-sequencing analyses in control and AFF3 knockdown IMR-90 cells. The results indicated that AFF3 knockdown leads to a partial reduction of DNA methylation at the *XIST* DMR, but not the tested AFF3 unbound region (Figure 5G and Supplementary Figure S6A–C). Therefore, our results suggest a role for the AFF3-DNA methylation pathway in regulating the *XIST* DMR in terminally differentiated cells.

Discussion

Silencing one of the two X chromosomes in mammalian females is initiated by mono-allelic activation of the lncRNA *XIST/Xist*. Once the process is triggered off in early embryogenesis, mono-allelic expression of *XIST/Xist* is maintained in almost all of cells in female (Lyon, 1961; Augui et al., 2011; Lee and Bartolomei, 2013). In this study, we have found a role of AFF3 in maintaining the mono-allelic expression of *XIST* gene. AFF3 can directly bind to the *XIST* DMR, located at the CpG island downstream of the *XIST* promoter in terminally differentiated cells. The binding of AFF3 to the *XIST* DMR depends on DNA methylation. Knockdown of AFF3 leads to upregulation of *XIST* transcript level and an increase in cells containing one more extra RNA cloud. Our results also suggest that ENL and AF9, which can interact with AFF3, might play similar roles in *XIST* gene silencing.

Our results show that AFF3 knockdown leads to upregulation of *XIST* RNA level. However, after AFF3 knockdown only a small percentage of cells display one more extra RNA clouds, as detected by RNA FISH. A possible explanation for this observation is that, in addition to upregulation of *XIST* RNA level, formation of *XIST* clouds requires various chromatin modify enzymes to create epigenetic landscapes, which favor *XIST* accumulation in cis on X chromosome (Simon et al., 2013; da Rocha et al., 2014).

We have previously reported that the recruitment of AFF3 to the imprinted gDMRs requires both DNA methylation and KAP1, a scaffold factor assembling H3K9me3 machinery at gDMRs (Quenneville et al., 2011; Luo et al., 2016). At the imprinted gDMRs, DNA methylation and H3K9me3 are interdependent. Deleting ZFP57, the Krüppel associated box (KRAB) domain containing zinc finger protein recruiting KAP1 and its associated H3K9me3 machineries to gDMRs, leads to both loss of H3K9me3 and DNA demethylation at gDMRs; H3K9me3 hallmarks at gDMRs are not maintained in DNA methylases DNMT1/3a/3b triple knockout cells (Quenneville et al., 2011). Therefore, the recruitment of AFF3 to the imprinted gDMRs requires both DNA methylation and KAP1 in mouse embryonic stem cells (Luo et al., 2016). In this study, we found that the binding of AFF3 to the *XIST* DMR mainly relies on DNA methylation, but not KAP1. It needs to be further investigated whether non-requirement of KAP1 in recruiting AFF3 to the *XIST* DMR is due to lack of

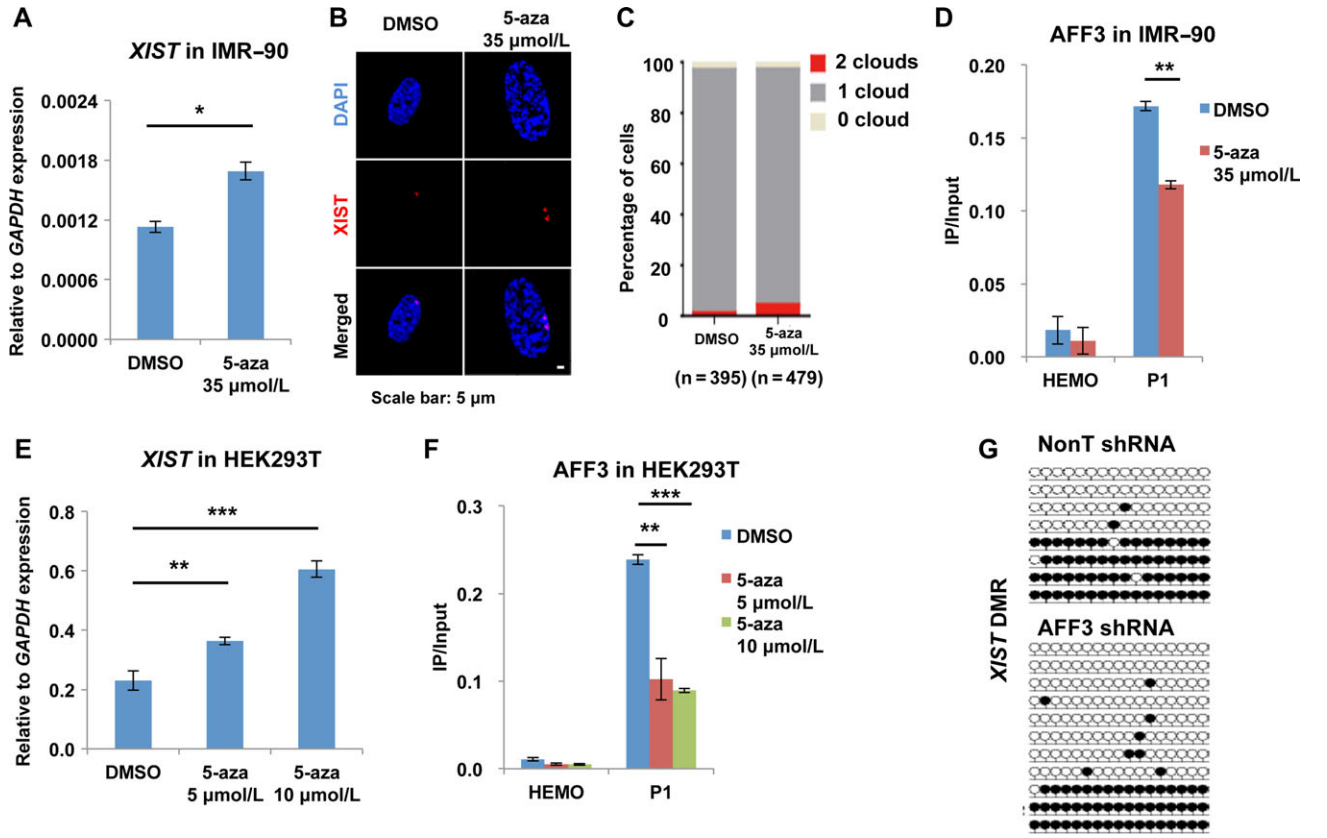

Figure 5 The recruitment of AFF3 to the *XIST* DMR is DNA methylation dependent. (**A**) RT-qPCR showing that *XIST* RNA level is increased after treating IMR-90 cells with the demethylating agent 5-aza. The expression of *XIST* was normalized to the expression of *GAPDH*. Results shown are technical replicates from representative biological replicates. (**B**) *XIST* RNA FISH in DMSO and 5-aza-treated IMR-90 cells. Scale bar, 5 μm. (**C**) Quantification of nuclei with *XIST* clouds in DMSO and 5-aza-treated IMR-90 cells. The Chi-square test shows that the difference of cells containing two *XIST* clouds between DMSO and 5-aza groups is significant. (**D**) ChIP-qPCR showing that 5-aza treatment in IMR-90 cells leads to a reduction of AFF3 occupancy at the *XIST* DMR. The *HEMO* gene served as a negative control for ChIP-qPCR. (**E**) RT-qPCR showing that *XIST* RNA level is increased after treating HEK293T cells with the demethylating agent 5-aza. The expression of *XIST* was normalized to the expression of *GAPDH*. Results shown are technical replicates from representative biological replicates. (**F**) ChIP-qPCR showing that 5-aza treatment in HEK293T cells leads to a reduction of AFF3 occupancy at the *XIST* DMR. The *HEMO* gene served as a negative control for ChIP-qPCR. (**A**, **D**, **E**, and **F**) Error bars represent standard deviations. Significant differences are marked with asterisks (*t*-test, $*P < 0.05$; $**P < 0.01$; $***P < 0.001$). (**G**) Bisulfite-sequencing analysis of DNA extracted from control and AFF3 knockdown IMR-90 cells at the *XIST* DMR. Methylated and unmethylated cytosines are designated by filled and unfilled circles, respectively. Each line indicates a unique DNA clone. The *XIST* DMR DNA methylation is slightly lost after AFF3 knockdown.

interdependency between DNA methylation and H3K9me3 at the *XIST* DMR, or due to KAP1 is not functioning as a scaffold for H3K9me3 machineries at the *XIST* locus.

Materials and methods

Cell culture

HEK293T cells were cultured in Dulbecco's modified Eagle medium (DMEM) supplemented with 10% fetal bovine serum (FBS) (ExCell Bio). IMR-90 cells were cultured in Eagle's Minimum Essential Medium (EMEM) supplemented with 10% FBS (Gibco). The cells were maintained under 5% CO_2 at 37°C. 5-aza (Sigma) was dissolved in dimethyl sulfoxide (DMSO) for a stock solution and added to the culture medium fresh on the day of the experiment.

Lentivirus-mediated RNAi

Human AFF3, ENL, AF9, KAP1, SETDB1, EHMT2, SUV39H1, and SUV39H2 shRNA constructs were cloned into the pLKO.1 vector (Addgene #10878). The non-targeting shRNA construct (SHC002) was purchased from Sigma. Packaging to get lentivirus particles and infection were performed as described previously (Luo et al., 2016). shRNA target sequences used in this study are listed in Supplementary Table S1. Briefly, HEK293T cells were plated in 150-mm culture plate and co-transfected with 8 μg of the shRNA construct or non-targeting shRNA construct, 6 μg of psPAX2 packaging plasmids, and 2 μg of pMD2.G envelope plasmids using Lipofectamine 2000 (Thermo Fisher Scientific) according to manufacturer's protocol. Lentiviral supernatants were collected 48 and 72 h after the transfection,

filtered through 0.45-μm filters. IMR-90 and HEK293T cells were infected with filtered lentiviral supernatants together with polybrene (Sigma) at the concentration of 8 μg/ml. Twenty-four hours after infection, the cells were subjected to selection with 1.5 μg/ml (IMR-90) and 2 μg/ml (HEK293T) of puromycin for additional 72 h, respectively.

Antibodies and western blot

The antibodies to 5-methyl-cytosine (5mC) (Eurogentec, BI-MECY-0100), KAP1 (Abcam, ab10484), and SETDB1 (Proteintech, 11231-1-AP) were purchased. Antibodies to AFF3 and AFF4 were described previously (Luo et al., 2012). A fragment of human AF9 (amino acids 406–498) was expressed as a His-tag fusion protein in pET-16b, purified on NTA-agarose according to Qiagen's protocol and by HPLC, and then sent to Genscript for immunization into rabbits. Whole-cell lysates for western blots were prepared by lysing cells in SDS-PAGE loading buffer.

qRT-PCR analysis

Total RNA was isolated with RNeasy kit (Qiagen), treated with RNase-free DNase I (New England Biolabs), and repurified with RNeasy columon. cDNAs were synthesized with the PrimeScript™ RT Master Mix (TaKaRa). The expression levels were measured with iTaq™ Universal SYBR® Green Supermix (Bio-Rad) on CFX96 (Bio-Rad). The relative expression levels of genes of interest were normalized to the expression of the housekeeping gene *GAPDH*. qRT-PCR primers used in this study are listed in the Supplementary Table S1.

RNA-Seq analysis

Reads from two biological replicates for each sample were aligned to the human genome UCSC hg19 and to gene annotations from Ensembl 67 using TopHat v2.0.9 (Trapnell et al., 2009). Cuffdiff v1.3.0 was used to quantify reads per kilobase million (RPKM) values, to perform differential expression analysis at FDR < 0.05, and to assess statistically sufficient read coverage for each gene (Trapnell et al., 2010). RNA-Seq reads were not extended for track figures and are shown at single base resolution.

ChIP and ChIP-Seq library preparation

ChIP assays were performed according to the previously described protocol (Lee et al., 2006). Briefly, a total of 5×10^7 HEK293T or IMR-90 cells were used per ChIP that cross-linked with 1% paraformaldehyde for 10 min at room temperature, and cross-linking was quenched by the addition of glycine. The fixed chromatin was sonicated into >200-bp fragments. Then 1% starting chromatin was saved as input sample. Immunoprecipitation with the specific antibodies was performed at 4°C overnight. The immune complex was collected by the protein A agarose beads and washed with RIPA buffer for five times. The chromatin was eluted, purified, and used as a template for qPCR or for ChIP-Seq libaray preparation. ChIP-qPCR primers used in this study are listed in the Supplementary Table S1. Libraries were prepared with NEBNext sample prep kit for the further next-generation sequencing.

ChIP-Seq analysis

ChIP-Seq reads were aligned to the human genome UCSC hg19 using the Bowtie aligner v0.12.9 allowing uniquely mapping reads only and allowing up to two mismatches (Langmead et al., 2009). Reads were extended to 150 bases toward the interior of the sequenced fragment and normalized to total reads aligned (reads per million; RPM). External sequencing data were acquired from GEO and Encode project as raw reads and aligned in the same way as internally sequenced samples. Peak detection was performed with MACS v1.4.2 (Zhang et al., 2008). Genome-wide sequencing datasets used in this study are listed in the Supplementary Table S2.

Bisulfite-sequencing analysis

Cell pellets were lysed in proteinase K digestion buffer (1 M Tris buffer, pH 8.0, 0.5 M EDTA, pH 8.0, 10% SDS) containing proteinase K at 50°C overnight. Genomic DNA was then isolated by phenol-chloroform method. The DNA samples were subjected to bisulfite treatment and purification using the EpiTect bisulfite kit (Qiagen). The purified DNA samples were then amplified using the primers corresponding to the *XIST* DMR and the AFF3 unbound region on Chromosome 21. Primers used for bisulfite-sequencing analysis are listed in the Supplementary Table S1. The PCR products were cloned into the pGEM-T easy vector (Promega). The clones were subjected to Sanger sequencing.

MeDIP

MeDIP assays were performed according to a previously described protocol (Ito et al., 2010). Briefly, The DNA fragments obtained with the specific antibody in ChIP were immunoprecipitated with the antibody against 5mC overnight at 4°C. MeDIP-qPCR primers used in this study are listed in the Supplementary Table S1.

RNA FISH

RNA FISH was performed according to Stellaris' RNA FISH protocol (Biosearch Technologies). Briefly, cells were grown on 18-mm round coverglass in a 12-well plate, fixed by 3.7% formaldehyde for 10 min, and permeabilized by 70% ethanol for at least 1 h. Cells were then washed with Wash Buffer A (Biosearch Technologies), and hybridized with 100 μl Hybridization Buffer (Biosearch Technologies) containing Stellaris XIST FISH probes for at least 4 h at 37°C in a humidified chamber. Coverglasses were mounted on slides in Vectashield containing DAPI and visualized under fluorescent microscope. RNA FISH combined with immunofluorescence was performed according to Stellaris' Sequential IF + RNA FISH protocol (Biosearch Technologies). Briefly, cells were grown on 18-mm round coverglass in a 12-well plate, fixed by 3.7% formaldehyde for 10 min, and permeabilized by 0.1% Triton X-100 in 1× PBS for 5 min. The cells were incubated with primary antibody for 1 h and then secondary antibody for another 1 h at room temperature, washed with PBS and fixed by 3.7% formaldehyde for

10 min. Cells were then washed with Wash Buffer A (Biosearch Technologies), and hybridized with 100 µl Hybridization Buffer (Biosearch Technologies) containing Stellaris XIST FISH probes for at least 4 h at 37°C in a humidified chamber. Coverglasses were mounted on slides in Vectashield containing DAPI and visualized under fluorescent microscope.

Supplementary material

Supplementary material is available at *Journal of Molecular Cell Biology* online.

Funding

This work was supported by Thousand Young Talents Plan of China (5631006003 to C.L., 6231000011 to Z.L.), Natural Science Foundation of Jiangsu Province of China (BK20160026 to C.L., BK20160666 and BK20170020 to Z.L.), and Fundamental Research Funds for the Central Universities (3231007201 to C.L., 3231008201 to Z.L.).

Conflict of interest: none declared.

References

Augui, S., Nora, E.P., and Heard, E. (2011). Regulation of X-chromosome inactivation by the X-inactivation centre. Nat. Rev. Genet. *12*, 429–442.

Borsani, G., Tonlorenzi, R., Simmler, M.C., et al. (1991). Characterization of a murine gene expressed from the inactive X chromosome. Nature *351*, 325–329.

Brockdorff, N., Ashworth, A., Kay, G.F., et al. (1991). Conservation of position and exclusive expression of mouse Xist from the inactive X chromosome. Nature *351*, 329–331.

Brown, C.J., Ballabio, A., Rupert, J.L., et al. (1991). A gene from the region of the human X inactivation centre is expressed exclusively from the inactive X chromosome. Nature *349*, 38–44.

Chen, D.L., Chen, L.Z., Lu, Y.X., et al. (2017). Long noncoding RNA XIST expedites metastasis and modulates epithelial-mesenchymal transition in colorectal cancer. Cell Death Dis. *8*, e3011.

Chureau, C., Chantalat, S., Romito, A., et al. (2011). Ftx is a non-coding RNA which affects Xist expression and chromatin structure within the X-inactivation center region. Hum. Mol. Genet. *20*, 705–718.

da Rocha, S.T., Boeva, V., Escamilla-Del-Arenal, M., et al. (2014). Jarid2 is implicated in the initial Xist-induced targeting of PRC2 to the inactive X chromosome. Mol. Cell *53*, 301–316.

de Araujo, E.S., Vasques, L.R., Stabellini, R., et al. (2014). Stability of XIST repression in relation to genomic imprinting following global genome demethylation in a human cell line. Braz. J. Med. Biol. Res. *47*, 1029–1035.

Gontan, C., Achame, E.M., Demmers, J., et al. (2012). RNF12 initiates X-chromosome inactivation by targeting REX1 for degradation. Nature *485*, 386–390.

Hansen, R.S., Canfield, T.K., Stanek, A.M., et al. (1998). Reactivation of XIST in normal fibroblasts and a somatic cell hybrid: abnormal localization of XIST RNA in hybrid cells. Proc. Natl Acad. Sci. USA *95*, 5133–5138.

Heard, E., Simmler, M.C., Larin, Z., et al. (1993). Physical mapping and YAC contig analysis of the region surrounding Xist on the mouse X chromosome. Genomics *15*, 559–569.

Ito, S., D'Alessio, A.C., Taranova, O.V., et al. (2010). Role of Tet proteins in 5mC to 5hmC conversion, ES-cell self-renewal and inner cell mass specification. Nature *466*, 1129–1133.

Jonkers, I., Barakat, T.S., Achame, E.M., et al. (2009). RNF12 is an X-Encoded dose-dependent activator of X chromosome inactivation. Cell *139*, 999–1011.

Langmead, B., Trapnell, C., Pop, M., et al. (2009). Ultrafast and memory-efficient alignment of short DNA sequences to the human genome. Genome Biol. *10*, R25.

Lee, J.T., and Bartolomei, M.S. (2013). X-inactivation, imprinting, and long noncoding RNAs in health and disease. Cell *152*, 1308–1323.

Lee, T.I., Johnstone, S.E., and Young, R.A. (2006). Chromatin immunoprecipitation and microarray-based analysis of protein location. Nat. Protoc. *1*, 729–748.

Lee, J.T., and Lu, N. (1999). Targeted mutagenesis of Tsix leads to nonrandom X inactivation. Cell *99*, 47–57.

Luo, Z., Lin, C., Guest, E., et al. (2012). The SEC family of RNA Polymerase II elongation factors: gene target specificity and transcriptional output. Mol. Cell. Biol. *32*, 2608–2617.

Luo, Z., Lin, C., Woodfin, A.R., et al. (2016). Regulation of the imprinted Dlk1-Dio3 locus by allele-specific enhancer activity. Genes Dev. *30*, 92–101.

Lyon, M.F. (1961). Gene action in the X-chromosome of the mouse (Mus musculus L.). Nature *190*, 372–373.

Makhlouf, M., Ouimette, J.F., Oldfield, A., et al. (2014). A prominent and conserved role for YY1 in Xist transcriptional activation. Nat. Commun. *5*, 4878.

Migeon, B.R., Lee, C.H., Chowdhury, A.K., et al. (2002). Species differences in TSIX/Tsix reveal the roles of these genes in X-chromosome inactivation. Am. J. Hum. Genet. *71*, 286–293.

Navarro, P., Pichard, S., Ciaudo, C., et al. (2005). Tsix transcription across the Xist gene alters chromatin conformation without affecting Xist transcription: implications for X-chromosome inactivation. Genes Dev. *19*, 1474–1484.

Quenneville, S., Verde, G., Corsinotti, A., et al. (2011). In embryonic stem cells, ZFP57/KAP1 recognize a methylated hexanucleotide to affect chromatin and DNA methylation of imprinting control regions. Mol. Cell *44*, 361–372.

Simon, M.D., Pinter, S.F., Fang, R., et al. (2013). High-resolution Xist binding maps reveal two-step spreading during X-chromosome inactivation. Nature *504*, 465–469.

Sun, B.K., Deaton, A.M., and Lee, J.T. (2006). A transient heterochromatic state in Xist preempts X inactivation choice without RNA stabilization. Mol. Cell *21*, 617–628.

Tao, Y., Yen, M.R., Chitiashvili, T., et al. (2018). TRIM28-regulated transposon repression is required for human germline competency and not primed or naive human pluripotency. Stem Cell Reports *10*, 243–256.

Tian, D., Sun, S., and Lee, J.T. (2010). The long noncoding RNA, Jpx, is a molecular switch for X chromosome inactivation. Cell *143*, 390–403.

Tinker, A.V., and Brown, C.J. (1998). Induction of XIST expression from the human active X chromosome in mouse/human somatic cell hybrids by DNA demethylation. Nucleic Acids Res. *26*, 2935–2940.

Trapnell, C., Pachter, L., and Salzberg, S.L. (2009). TopHat: discovering splice junctions with RNA-Seq. Bioinformatics *25*, 1105–1111.

Trapnell, C., Williams, B.A., Pertea, G., et al. (2010). Transcript assembly and quantification by RNA-Seq reveals unannotated transcripts and isoform switching during cell differentiation. Nat. Biotechnol. *28*, 511–515.

Ui, A., and Yasui, A. (2016). Collaboration of MLLT1/ENL, Polycomb and ATM for transcription and genome integrity. Nucleus *7*, 138–145.

Wang, Y., Shen, Y., Dai, Q., et al. (2017). A permissive chromatin state regulated by ZFP281-AFF3 in controlling the imprinted Meg3 polycistron. Nucleic Acids Res. *45*, 1177–1185.

Yildirim, E., Kirby, J.E., Brown, D.E., et al. (2013). Xist RNA is a potent suppressor of hematologic cancer in mice. Cell *152*, 727–742.

Zhang, Y., Liu, T., Meyer, C.A., et al. (2008). Model-based analysis of ChIP-Seq (MACS). Genome Biol. *9*, R137.